Continuous Spacecraft Communications via Make-Before-Break Antenna Array Beam Steering

Adam Gannon†, Bryan Schoenholz, James Downey, John Clapham
Communications & Intelligent Systems Division, NASA Glenn Research Center
Cleveland, Ohio, USA
†adam.gannon@nasa.gov

***Abstract*—Active phased array (APA) antennas can electronically form multiple beams to track several targets simultaneously. Spacecraft equipped with these antennas can achieve continuous communications through a constellation of relay satellites by forming a second beam to an upcoming relay satellite before the spacecraft moves beyond the current relay's line of sight. These make-before-break operations have utility for streaming critical data without gaps. Using characterization data from a commercially-available APA-based satellite communications terminal, we simulate performance from low-Earth orbit to a representative geosynchronous relay satellite system at Ka-band. Average data rates of 3 Mbps are achievable with a minimum rate of 0.8 Mbps during worst-case handovers. We prototype the beam-splitting algorithm in the terminal hardware and evaluate its performance in an antenna range. In an over-the-air test emulating a handover between two relays we observe error-free data in the combined telemetry stream.**

***Index Terms*—active phased array antennas, space communications, make-before-break, beam steering, relay satellites**

I. Introduction

Spacecraft performing science and exploration objectives desire low-latency communications pathways for telemetry, commanding, and high-priority data transfer [1], [2]. Constellations of space relay satellites offer connectivity to entire orbital planes particularly in low-Earth orbit (LEO). Commercial relays servicing the next-generation of space missions will be required to provide near-continuous availability for critical communications [3]. However, an orbiting spacecraft utilizing body pointing or a single mechanically-steered dish must break connection to a receding relay in order to train its antenna on an upcoming relay. Additionally, gimbal motion imparts microvibrations on the spacecraft structure which can perturb measurements [4], [5]. This is particularly true for high-precision optical instruments which require maintaining milli-arc-second pointing accuracy to a target [6].

Active phased array (APA) antennas offer near-instantaneous electronic steering with no moving parts. A single APA can form dual beams which can simultaneously track the receding and upcoming relays during a handover. This make-before-break operation allows continuous communications for critical telemetry. However, adoption of APA-based terminals on space vehicles performing scientific observations has historically been hindered by high per-unit costs of bespoke chipsets suitable for bands in the satellite service. Recent years have seen substantial increase in the availability of beamforming chips driven by Fifth Generation (5G) mobile broadband base stations. In particular, the frequency range of chipsets manufactured for the n258 band (24.25-27.5 GHz) overlaps significantly with Ka-band spectrum used by space missions. Leveraging commercial timescales and production volumes, user terminals based on these devices offer the capability benefits of APAs at substantially reduced costs [7], [8].

Several APA architectures exist to support multiple beams. In the simplest case, an analog combiner network shapes several beams from a single RF signal – each beam containing the same data. Other hybrid or fully-digital designs include additional combiner networks capable of generating beams with individual signals at the cost of additional complexity and power consumption [9]. Since protocols common in satellite downlinks generally do not require handshaking, it is not necessary to have an independent data stream in a second beam. In this case, arrays using a simple analog beamforming scheme can send the same signal towards two relays during a handover period to maintain connectivity. Though conceptually straightforward, there exists little work in the literature which provides robust analysis of the technique and its expected performance in space.

In this work, we demonstrate dual-beam steering from a commercially-available space-grade APA in an over-the-air handover emulation. We present simulation results which show feasibility of continuous communications from a mission in LEO utilizing an APA. Electronic steering of two beams allows the upcoming relay satellite to acquire the mission's signal before line of sight to the current relay is lost. After the handover is complete, a single beam tracks the active satellite until the next handover period. Physical layer protocols with variable modulation allow the spacecraft to adjust data rate in line with varying signal strength [10], [11]. This process repeats, providing the satellite with continuous communications coverage.

II. Motivation

Consider an example scenario of a LEO spacecraft communicating through a four-satellite relay constellation in geosynchronous orbit. As a representative spacecraft we use the two-line elements (TLEs) of the International Space Station (ISS) and four of NASA's Tracking and Data Relay Satellites (TDRS): TDRS-8, 9, 10, and 13[1]. The zenith-mounted array is capable of electronic steering to $\pm 60^\circ$ with a usable pattern out to $\pm 75^\circ$. Line-of-sight calculations performed in an orbital mechanics and communications analysis tool [13] over a simulation period of three months show windows of 100–1,500 seconds during which the spacecraft can simultaneously view two relays (Fig. 1). By performing make-before-break handovers during these periods, a dual-beam APA can achieve uninterrupted orbital coverage.

Antenna	Max Slew Rate	Coverage
Dual-Beam APA	Near-Instantaneous	100%
ISS SGANT [14]	3°/sec [15]	97.3%
SCaN Testbed [16]	1°/sec [17]	91.8%

TABLE I
POTENTIAL COVERAGE IN FOUR-RELAY SCENARIO DUE TO SLEW RATE LIMITATIONS FOR TWO REPRESENTATIVE GIMBALED DISHES. STATISTICS OVER A THREE MONTH SIMULATION.

For comparison, in Table I we simulate the performance of two representative gimbaled dishes flown on ISS. At a handover period beginning when the angular separation between receding and upcoming satellites is minimized, we calculate the duration of gimbal movement as a function of slew rate. An average gap of 40 and 121 seconds per handover is found for slew rates of 3°/sec and 1°/sec, respectively. The sum of gaps represents a 3–8% loss of the spacecraft's communications coverage.

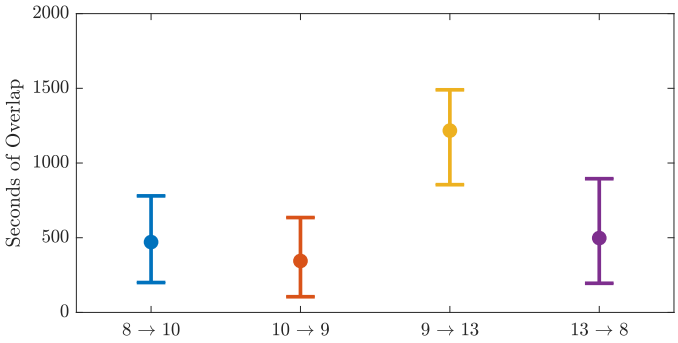

Fig. 1. Overlap in line of sight to four TDRS relays from an APA on a LEO user spacecraft with $\pm 75^\circ$ steering. Statistics simulated over three months.

III. System Operations

A. Steering Calculations

The make-before-break handover process begins with knowledge of angles towards the receding (θ_r, ϕ_r) and upcoming (θ_u, ϕ_u) relay satellites for each discrete time step t during the handover window defined by $[t_{\text{start}}, t_{\text{stop}}]$. These can be uplinked from a mission operations center in advance or a spacecraft with position knowledge of itself and the relay satellites can perform the computation onboard [18].

[1]TLEs gathered for this simulation reflect TDRS locations as of November 2022. TDRS-9 has since been retired [12].

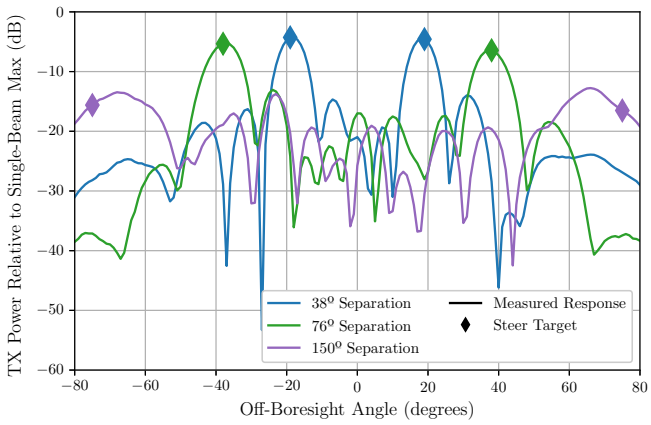

Fig. 2. Far field cuts ($\phi = 0$) of APA dual-beam radiation pattern at representative separations between beams.

The elements of an APA form a grid of $M \times N$ elements with inter-element spacing of d_x and d_y in the horizontal and vertical directions, respectively. For descriptive simplicity, we will not consider offsets between rows or absent elements, though the algorithm deployed on the hardware contains additional steps to compensate for both. During a handover, the APA forms two beams towards (θ_r, ϕ_r) and (θ_u, ϕ_u) by setting the phase and amplitude of each antenna element. Let $AF(\theta, \phi)$ indicate the array factor

$$AF(\theta, \phi) = \sum_{m=0}^{M-1} \sum_{n=0}^{N-1} a_{mn} e^{jk(md_x u + nd_y v)} \tag{1}$$

where $u = \sin\theta\cos\phi$, $v = \sin\theta\sin\phi$, and $k = 2\pi/\lambda_c$ for carrier wavelength $\lambda_c = c/f_c$ [19]. Single-beam steering towards target (θ_i, ϕ_i) is accomplished by setting the complex weight of the (m, n)th element as

$$a_{mn}(\theta_i, \phi_i) = |a_{mn}| e^{-jk(md_x u_i + nd_y v_i)}. \tag{2}$$

For dual beams of equal power the weights are set as

$$a_{mn} = \frac{1}{\sqrt{2}}[a_{mn}(\theta_r, \phi_r) + a_{mn}(\theta_u, \phi_u)]. \tag{3}$$

In practice, beam steering involves commanding a gain of $20\log_{10}|a_{mn}|$ dB and phase $\angle a_{mn}$ to each (m, n)th antenna element. This process is repeated for the duration of the handover as summarized in Algorithm 1. APA hardware may allow a series of pre-computed beam states to be stored in memory in advance of the handover for lower latency. In this case, software will command the APA to load each beam state from memory in turn during the handover.

Fig. 2 shows several representative far field cuts of dual beam steering on a CesiumAstro APA-1AT1 transmitting in the Ka-band ($f_c = 27$GHz) with $\phi = 0^\circ$ and $\theta = \pm[19^\circ, 38^\circ, 75^\circ]$.

Algorithm 1 Beam steering calculation around handover.

while $t < t_{\text{start}}$ **do** ▷ Before handover
  Compute (θ_r, ϕ_r).
  $a_{mn}(\theta_r, \phi_r) \leftarrow |a_{mn}| e^{-jk(md_x u_r + nd_y v_r)}$
while $t_{\text{start}} \leq t \leq t_{\text{stop}}$ **do** ▷ Dual-beam active
  Compute (θ_r, ϕ_r) and (θ_u, ϕ_u).
  $a_{mn}(\theta_r, \phi_r) \leftarrow |a_{mn}| e^{-jk(md_x u_r + nd_y v_r)}$
  $a_{mn}(\theta_u, \phi_u) \leftarrow |a_{mn}| e^{-jk(md_x u_u + nd_y v_u)}$
  $a_{mn} \leftarrow \frac{1}{\sqrt{2}}[a_{mn}(\theta_r, \phi_r) + a_{mn}(\theta_u, \phi_u)]$
while $t > t_{\text{stop}}$ **do** ▷ Handover complete
  Compute (θ_u, ϕ_u).
  $a_{mn}(\theta_u, \phi_u) \leftarrow |a_{mn}| e^{-jk(md_x u_u + nd_y v_u)}$

Beamforming is accurate within the $\pm 60°$ specification of the device. However, we can reasonably steer to $\pm 75°$ with some additional loss by operating off the beam's peak. Scan loss of the device is characterized in Fig. 3. Variation over azimuth becomes more significant beyond the $\pm 60°$ specification and results in ± 1 dB difference from the $10 \log_{10} \cos^{1.31}(\theta)$ best-fit.

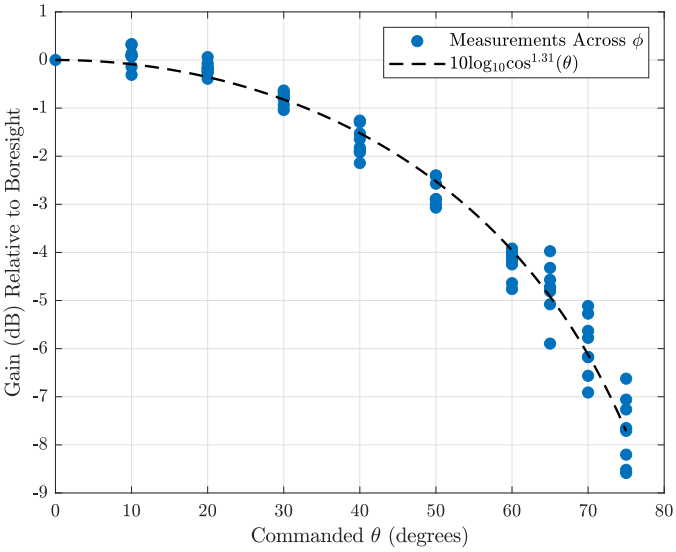

Fig. 3. Scan loss of APA with ϕ varied over $[0°, 315°]$ in $45°$ steps.

B. Rate Adaptation

We desire a physical-layer protocol suited to signal variations, particularly one capable of reducing rate to maintain connectivity during handover periods. We consider the 2nd Generation Digital Video Broadcasting – Satellite standard and its extensions (DVB-S2X) [20]. Within a fixed symbol rate configuration, DVB-S2X allows the spacecraft to vary data rate by changing modulation and coding (MODCOD) on a frame-by-frame basis. A feedback link can enable closed-loop adaptation in real time or a variable MODCOD profile can be pre-computed and run open loop. Using the Generic Stream Encapsulation (GSE) protocol [21] one or several IP packets can be encapsulated in each frame allowing variable-rate traffic to flow from the spacecraft to Earth.

The duration of handovers must be decided based on link performance. This period must be long enough to reliably acquire the signal through the upcoming relay but aim to minimize the time during which two assets are occupied supporting the same mission. We performed laboratory tests with the Newtec MDM6000 DVB-S2X modem operating at a representative symbol rate of 1.5 Mbaud and lowest DVB-S2X MODCOD. A noise generator set the signal C/N_0 to 63 dB-Hz which corresponds to a realistic signal level during handover. Across 10 trials the modem consistently acquired within 10 seconds. This period is selected for the handover duration used in the subsequent range experiments and simulations. In operations, this would determine the times for each contact in the relay satellite system's schedule to provide overlap. However, we note lock time performance must be thoroughly characterized for each provider's specific modem at anticipated signal levels.

IV. Range Experiment

To evaluate algorithmic performance in hardware, we performed emulated handovers in a testbed at NASA Glenn Research Center [22]. An anechoic chamber (Fig. 4) houses the hardware for over-the-air tests. The APA is a CesiumAstro Nightingale-1 terminal which includes the 186-element APA-1AT1 packaged with a single-board computer, software-defined radio, power conditioning unit, and up/down converter. The terminal is mounted in a Pumpkin Supernova 6U CubeSat structure of which it occupies approximately 1U (a cube with 10 cm sides) in volume. The exterior face with the APA mounted also contains an S-band patch antenna and sun sensor – a similar configuration as the Cesium Mission 1 flight [23]. The CubeSat is mounted on a two-axis gimbal whose motion emulates satellite movement relative to the relays during an orbit. Two horn antennas placed in the far field act as the receding and upcoming relay satellites. Space limitations inside the anechoic chamber allow the horns to be

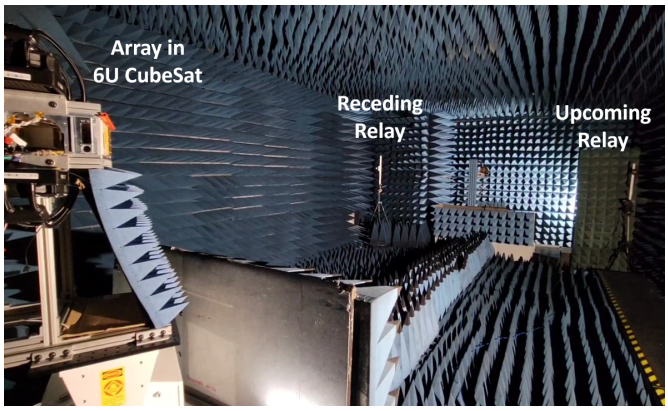

Fig. 4. Emulation testbed in anechoic chamber at Glenn Research Center. Two receive horns in the far field (approximately 6.5m) act as relay satellites.

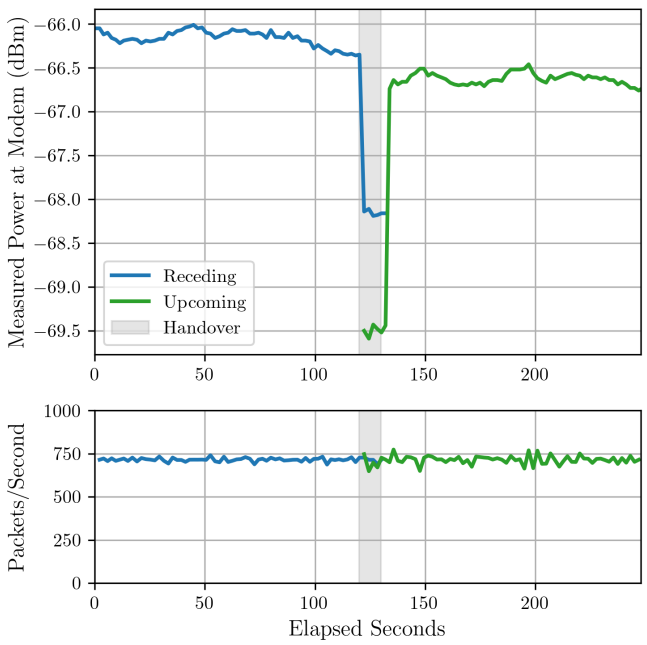

Fig. 5. Measurements at emulated relays during handover. Received power (top) is approximately constant besides a ∼3dB reduction as the beam is split. Error-free packet rate (bottom) remained constant with an overlap during the handover period.

separated by a maximum of 38°. A dual beam pattern to both receivers should resemble the trace in Fig. 2.

We emulate a handover by moving from $-31°$ to $+31°$ over 248 seconds, centered around the midpoint (0°) between relays. The gimbal moves at 0.5°/sec. As will be seen in Section V, this rate is more than sufficient to emulate the angular motion of the spacecraft relative to relay satellites in several representative scenarios. Beamforming software on the APA executes open loop independently of gimbal control to emulate the on-orbit environment. Each horn is connected to an independent downconverter which translates the 27 GHz frequency to 1.2 GHz. Each signal is in turn connected to an independent MDM6000 modem which performs demodulation and forwarding of GSE-encapsulated IP traffic to an emulated mission operations center. Adjusting for the short antenna range distance, we operate the APA at an EIRP of -9 dBW. Modulation order is selected to produce a 16 dB link margin to a horn when tracked by a single beam (13 dB at handover) and negative link margin when the APA targets the other receiver. We do not employ adaptive modulation in this test since path loss throughout the emulated contact will remain static.

Fig. 5 plots the input power to the modems over the 248 second test duration. We observe power during single beam periods is roughly flat with some variation due to scan loss. The receding modem receives error free data at approximately 720 packets per second up to and including during the entire handover period. The handover occurs between 120–130 s. The upcoming modem locks at 123 s and produces error-free data for the rest of the contact. There is a 7 s period where both receive data simultaneously before the APA returns to a single beam and signal to the receding relay is lost.

V. Simulation

A. GEO Scenario

To predict performance in space, we begin with a simulation of the LEO-TDRS scenario described in Section II. Angular motion of the spacecraft with respect to the four TDRS relays is a maximum of 0.12°/sec. As shown in Section IV, the spacecraft beamforming software can easily handle this rate.

The simulated spacecraft is assumed to use the CesiumAstro Nightingale-1 terminal from Section IV with scan loss as measured in Fig. 3. The terminal operates with an EIRP of 30 dBW at P_{1dB} [24]. We use receiver specifications for the Ka-capable 2nd and 3rd generation TDRS [25] and an operational frequency of $f_c = 27$ GHz. These link budget parameters, summarized in Table II, are used to compute C/N_0 to each relay considering a single beam.

As shown in Fig. 6, line of sight dictates the possible handover window, though the optimal time occurs about the intersection of the two curves when the signal to each relay is strongest. Splitting the beam will decrease power received at each relay by 3 dB. Additionally, variations in scan loss and free-space path loss will vary signal levels by a further 2–8 dB over the contact.

Parameter	Value
Spacecraft EIRP	30 dBW [24]
Relay G/T	26.5 dB/K [25]
Center Frequency	27 GHz
Link Margin	2 dB

TABLE II
Link Budget Parameters for Four-Relay LEO Scenario.

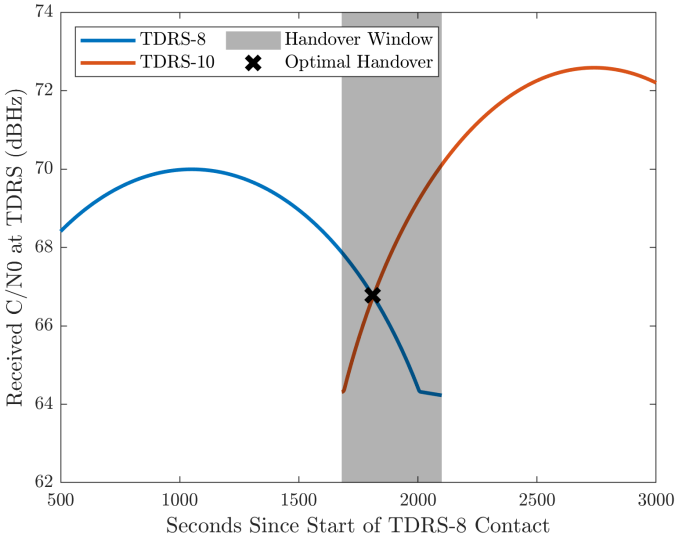

Fig. 6. C/N_0 profiles to receding (TRDS-8) and upcoming (TDRS-10) relays in example scenario. Shaded area indicates visibility window for potential handovers. Optimal handover occurs when both signals are strongest.

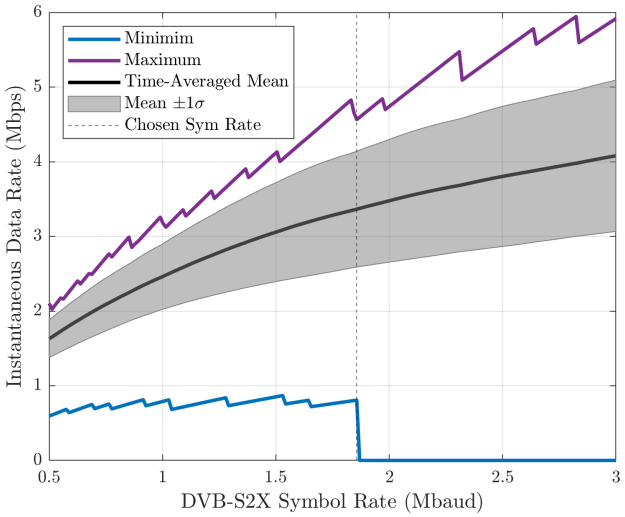

Fig. 7. Data rate as a function of symbol rate for the LEO-TDRS scenario. The dashed line indices the symbol rate which maximizes average data rate. Statistics over three months.

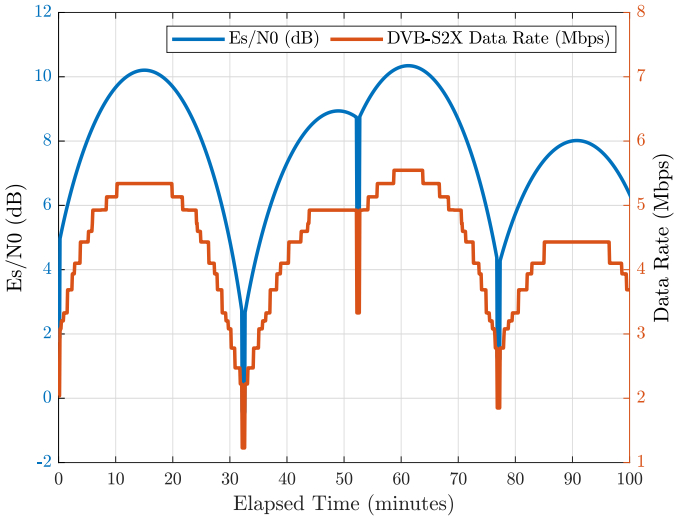

Fig. 8. Time-varying data rate and E_S/N_0 across three simulated handovers at selected 1.86 Mbaud symbol rate. The DVB-S2X MODCOD selection includes a 2 dB margin above quasi error-free thresholds in the standard.

To select optimal DVB-S2X symbol rate we perform a three month simulation containing more than 5,000 handovers. Handover duration is assumed to be the 10 seconds from Section III-B. Symbol rate is fixed for the simulation duration and data rate is calculated by selecting the set of modulation and coding with the highest bits per symbol while maintaining 2 dB of margin above the quasi error-free E_S/N_0 thresholds presented in the standard [20]. Fig. 7 shows the minimum data rate as a function of selected symbol rate. We find 1.86Mbaud is the highest symbol rate for which the link closes over the entire simulation period including handovers. At a typical roll-off of 35% this represents an occupied bandwidth of 2.51 MHz.

Over the three month simulation selected MODCOD varies from QPSK 2/9 (the lowest in the standard) to 16APSK 28/45. The maximum gapless symbol rate of 1.86 Mbaud results in a time-averaged mean rate of 3.37 Mbps and a minimum rate of 0.81 Mbps. The rate within one standard deviation ranges 2.59–4.14 Mbps. This is significantly higher than the minimum rate because handovers are short compared to the duration of contacts. This is illustrated in Fig. 8 which plots signal conditions and chosen MODCOD over three representative handovers in the simulation. We observe a steep drop in rate corresponding with the 3 dB lower E_S/N_0 during the handover. However, this short low-rate period is immediately followed by a rate increase of at least 1 Mbps as the handover is complete and the APA returns to forming a single beam. Within the 20–30 minute relay contact, data rate adjusts to the time-varying path loss and scan loss.

While this 1.86 Mbaud operating point does maximize the average data rate it does not produce the highest minimum data rate. This occurs at a symbol rate of 1.54 Mbaud which yields a minimum rate of 0.88 Mbps but an average rate of 3.10 Mbps. A mission's priorities may prefer one operating point over another. Finally, the Nightingale-1 architecture supports combination of multiple APA tiles, with each doubling in aperture resulting in a 6 dB increase in EIRP. We predict a quad-tile APA in this scenario would produce average data rates of 53.8 Mbps.

B. MEO Scenario

Simulated performance was also computed for the LEO spacecraft communicating with a constellation of relay satellites in medium Earth orbit (MEO). For a representative system we used TLEs of the SES O3b MEO constellation. Twenty relays in equatorial orbit comprise the constellation of which our simulation uses 15 which occupy unique orbital slots. The relay field of view is optimized for visibility to latitudes within 45° of the equator [26] with extended coverage up to 62° [27]. Since MEO is closer to Earth (approximately 8,000 km altitude as opposed to 35,000 km for TDRS) it makes sense to position the APA on a face of the spacecraft aligned with the velocity vector (i.e. ram-facing) instead of zenith-facing as before.

As in the GEO scenario, electronic dual-beam steering enables continuous communications coverage over the spacecraft's entire orbit. The denser constellation results in more handovers and shorter contacts to a single satellite on the order of 5–15 minutes. Maximum relative angular motion is 0.21°/sec. A representative G/T parameter was estimated for use in the simulation. The highest symbol rate which provides gapless coverage is 0.39 Mbaud. This results in a

Parameter	GEO	MEO
Num. Relays in Scenario	4	15
APA Orientation	Zenith	Ram
Average Handovers Per Day	58	158
Time-Averaged Data Rate	3.37 Mbps	0.50 Mbps
Data Rate Range	0.17–0.76 Mbps	0.81–4.60 Mbps

TABLE III
COMPARISON BETWEEN GEO AND MEO SCENARIO SIMULATIONS.

time-averaged data rate of 0.50 Mbps and minimum rate of 0.17 Mbps. This lower rate is expected since apertures of commercial MEO relays are assumed to be smaller than the quite large 4.9 m single-access antennas on TDRS. Table III summarizes key parameters for both simulations.

VI. Conclusion

The approach demonstrated in this work is generally applicable to APAs forming dual beams from a single RF signal (as in this experiment) or multiple beams each containing an independent signal. Though our primary example scenario considered the TDRS system, this approach is equally applicable to any non-regenerative ("bent pipe") relay satellite system. An APA forming multiple beams with independent RF signals would be most useful with systems which require handshaking or authentication before data transfer can begin. However, the single-signal approach still has some utility here as well since the upcoming relay can begin to train receiver loops on the RF signal to reduce acquisition time before handshaking can begin. Any APA-based communication terminal with sufficient link margin, ability to vary data rate, and line of sight to relays should be able to benefit from this approach for continuous communications.

VII. Acknowledgments

We thank Christine Chevalier for her software development of the gimbal control. Nick Varaljay and Kevin Lambert prepared the test setup in the anechoic chamber including CubeSat mounting. David Brooks was critical in configuring networking required to flow IP traffic. This work was performed under the SmallSat Ka-band Operations User Terminal (SKOUT) project, funded by NASA's Space Communications and Navigation program.

References

[1] K. J. Murphy *et al.*, "LANCE, NASA's land, atmosphere near real-time capability for EOS," in *Time-Sensitive Remote Sensing*. New York, NY: Springer New York, 2015.

[2] F. H. Stillwagen, "Communications and tracking of visiting vehicles near ISS: The design of the reusable launch vehicle communications," NASA Langley Research Center, Tech. Rep., Apr. 1999.

[3] "Communications services project (CSP) announcement for proposals (AFP)," July 2021, NASA Solicitation NNC21AFP01R.

[4] M. Vitelli, B. Specht, and F. Boquet, "A process to verify the microvibration and pointing stability requirements for the bepicolombo mission," in *Proc. 1st Int. Workshop Instrumentation for Planetary Missions*, Greenbelt, MD, Aug. 2012.

[5] I. G. Moneva, B. Kunicka, R. Schweikle, M. Oettrich, and H. Langenbach, "Design and test results of a microvibration improvement for an antenna pointing mechanism," in *Proc. 18th European Space Mechanisms and Tribology Symp.*, Munich, Germany, Sep. 2019.

[6] L. Li, L. Wang, L. Yuan, R. Zheng, Y. Wu, J. Sui, and J. Zhong, "Microvibration suppression methods and key technologies for high-precision space optical instruments," *Acta Astronautica*, vol. 180, pp. 417–428, 2021.

[7] J. A. Nessel, J. M. Downey, B. L. Schoenholz, M. T. Piasecki, and F. A. Miranda, "Potential applications of active antenna technologies for emerging NASA space communications scenarios," in *14th European Conf. Antennas and Propagation (EuCAP)*, Virtual, Mar. 2020.

[8] A. Gannon, J. Downey, and B. Schoenholz, "Towards Gbps downlinks from low-cost active phased arrays," in *2024 IEEE Space Hardware and Radio Conf. (SHaRC)*, San Antonio, TX, Jan. 2024.

[9] I. Ahmed, H. Khammari, A. Shahid, A. Musa, K. S. Kim, E. De Poorter, and I. Moerman, "A survey on hybrid beamforming techniques in 5G: Architecture and system model perspectives," *IEEE Communications Surveys & Tutorials*, vol. 20, no. 4, pp. 3060–3097, 2018.

[10] G. Albertazzi *et al.*, "On the adaptive DVB-S2 physical layer: design and performance," *IEEE Wireless Communications*, vol. 12, no. 6, pp. 62–68, 2005.

[11] J. Downey, D. Mortensen, M. Evans, J. Briones, and N. Tollis, "Adaptive coding and modulation experiment using NASA's space communication and navigation testbed," in *34th AIAA International Communications Satellite Systems Conference*, Cleveland, OH, Oct. 2016.

[12] "Nasa's tracking and data relay satellite-9 reaches end of mission," nasa.gov/feature/nasa-TDRS-9-end-of-mission.

[13] J. M. Shah and B. W. Welch, "Space communications and navigation (SCaN) tool capabilities updates for antenna pattern and jitter," NASA Glenn Research Center, Tech. Rep. NASA/TM—2019-220233, 2019.

[14] X. Zhang, "ISS SGANT group level offloading test mechanism," in *Proc. 36th Aerospace Mechanisms Symp.*, Cleveland, OH, May 2002.

[15] K. Jules, K. Hrovat, E. Kelly, and T. Reckart, "International space station increment–6/8 microgravity environment summary report," NASA Glenn Research Center, Tech. Rep. NASA/TM—2006-213896, 2006.

[16] D. Mortensen, R. Reinhart, S. Johnson, J. Briones, and D. Chelmins, "The space communications and navigation testbed aboard international space station: Seven years of space-based reconfigurable software defined communications, navigation, and networking," in *ISS Research and Development Conf.*, Atlanta, GA, July 2019.

[17] B. Welch, former SCaN Testbed RF/communications lead, email correspondance on Nov. 11, 2021.

[18] A. Gannon, C. Gemelas, S. Paulus, D. Schrage, L. Vincent, and C. Roberts, "An augmented ground station architecture for spacecraft-initiated communication service requests," in *16th Int. Conf. Space Operations (SpaceOps)*, Virtual, May 2021.

[19] R. J. Mailloux, *Phased Array Antenna Handbook*. Norwood, MA: Artech House, 2005.

[20] "Digital video broadcasting (DVB) second generation part 2: DVB-S2 extensions (DVB-S2X)," European Telecommunications Standards Institute, Standard ETSI EN 302 307 v1.2.1, May 2020.

[21] "Digital video broadcasting (DVB) generic stream encapsulation (GSE)," European Telecommunications Standards Institute, Standard ETSI TS 102 606-1 v1.2.1, Jul 2014.

[22] J. Nessel, J. Downey, and C. Niederhaus, "The multiple access testbed for research in innovative communications systems (MATRICS)," in *ESA Antenna Workshop*, Noordwijk, Netherlands, Oct. 2018.

[23] "Cesium mission 1," cesiumastro.com/old/cesium-mission-01.

[24] "Nightingale-1 specifications," cesiumastro.com/systems/nightingale1.

[25] M. Toral, G. Heckler, P. Pogorelc, N. George, and K. Han, "Payload performance of third generation TDRS and future services," in *Int. Communications Satellite Systems Conf. (ICSSC)*, Trieste, Italy, Oct. 2017.

[26] S. H. Blumenthal, "Medium earth orbit ka band satellite communications system," in *IEEE Military Communications Conf. (MILCOM)*, San Diego, CA, Nov. 2013.

[27] J. P. Connolly, "Technique for geolocation of EMI emitters by O3B satellites," M.S. thesis, Naval Postgraduate School, Monterey, CA, June 2016.